Biomatter 4, e29506; June 2014; © 2014 Landes Bioscience

Design of 2D chitosan scaffolds via electrochemical structuring

Lina Altomare[1,2,*], Elena Guglielmo[1], Elena Maria Varoni[3], Serena Bertoldi[1,2], Andrea Cochis[4], Lia Rimondini[4], and Luigi De Nardo[1,2]

[1]Politecnico di Milano; Department of Chemistry, Materials, and Chemical Engineering; Milan, Italy; [2]INSTM - Consorzio Interuniversitario Nazionale per la Scienza e Tecnologia dei Materiali; Local Unit Politecnico di Milano; Milan, Italy; [3]Clinica Odontoiatrica A.O. San Paolo Università degli Studi di Milano; Milan, Italy; [4]Università del Piemonte Orientale "Amedeo Avogadro"; Department of Health Sciences; Laboratory of Biomedical and Dental Materials; Novara, Italy

Keywords: micropattern, chitosan, genipin, epichlorohydrin, electrochemical deposition

Chitosan (CS) is a versatile biopolymer whose morphological and chemico-physical properties can be designed for a variety of biomedical applications. Taking advantage of its electrolytic nature, cathodic polarization allows CS deposition on electrically conductive substrates, resulting in thin porous structures with tunable morphology. Here we propose an easy method to obtain CS membranes with highly oriented micro-channels for tissue engineering applications, relying on simple control of process parameters and cathodic substrate geometry.

Cathodic deposition was performed on two different aluminum grids in galvanostatic conditions at 6.25 mA cm^{-2} from CS solution [1g L^{-1}] in acetic acid (pH 3.5). Self-standing thin scaffolds were cross linked either with genipin or epichlorohydrin, weighted, and observed by optical and electron microscopy. Swelling properties at pH 5 and pH 7.4 have been also investigated and tensile tests performed on swollen samples at room temperature. Finally, direct and indirect assays have been performed to evaluate the cytotoxicity at 24 and 72 h.

Thin scaffolds with two different oriented porosities (1000μm and 500μm) have been successfully fabricated by electrochemical techniques. Both cross-linking agents did not affected the mechanical properties and cytocompatibility of the resulting structures. Depending on the pH, these structures show interesting swelling properties that can be exploited for drug delivery systems. Moreover, thanks to the possibility of controlling the porosity and the micro-channel orientation, they should be used for the regeneration of tissues requiring a preferential cells orientation, e.g., cardiac patches or ligament regeneration.

Introduction

Most human tissues have a limited regeneration potential after damage: their recovery, in terms of both structure and function, is often incomplete, usually leading to scar formation and impaired functionality.[1] With the advent of tissue engineering, exogenous strategies are gaining increasing attention as a valuable option to find solutions for the incomplete regeneration of different tissues.[2,3] Both in vitro and in vivo scaffold mediated tissue engineering approach—to reconstruct tissues—and the in vivo delivery of cells—to induce endogenous tissue regeneration—are emerging as potential therapeutic goals.[1]

Biomaterial selection as well as material processing into a 3D structure becomes hence increasingly important not only to attain an environment correctly addressing cell fate and tissue development,[1] but also to encourage widespread clinical application. Developmental aspects of cells, such as growth, differentiation, migration, and maturation have been taken into account to design substrate properties like degradation, porosity, fibrous structure, ability to adsorb and release bioactive factors: along this direction, several materials and processing approaches have been investigated.[4-6] Among them chitosan-based scaffolds possess some unique properties supporting their use for tissue engineering. First, chitosan can be formed in different structures such as interconnected-porous structures, fibers, hydrogels; second, the cationic nature of chitosan also allows for pH-dependent electrostatic interactions with anionic glycosaminoglycans (GAG) and proteoglycans, widely distributed throughout the body, and other negatively charged species. This latter property is extremely important because a number of cytokines and growth factors are known to be bound to and modulated by GAG.[7] Finally chitosan has been successfully used in different advanced tissue regeneration applications. For example, it has been demonstrated that temperature-responsive chitosan hydrogels are suitable matrices for cardiomyocytes transplantation,[8] and chitosan hydrogels can be also used as injectable cells delivery system to improve myocardial performances of infarcted heart.[9]

Together with mechanical and chemico-physical properties, topographic cues are particularly important in determining cell phenotypes, especially for tissues that are highly dependent on

*Correspondence to: Lina Altomare; Email: lina.altomare@polimi.it
Submitted: 02/05/2014; Revised: 05/23/2014; Accepted: 06/05/2014; Published Online: 06/18/2014
http://dx.doi.org/10.4161/biom.29506

Table 1. Samples abbreviations

Abbreviation	Explanation
EPI 1000	Chitosan meshes having micro-channels of 1000 µm diameter, cross-linked with Epichloroydrin
EPI 500	Chitosan meshes having micro-channels of 500 µm diameter, cross-linked with Epichloroydrin
EPI Random	Chitosan meshes having random porosity, cross-linked with Epichloroydrin
GEN 1000	Chitosan meshes having micro-channels of 1000 µm diameter, cross-linked with Genipin
GEN 500	Chitosan meshes having micro-channels of 500 µm diameter, cross-linked with Genipin
GEN Random	Chitosan meshes having a random porosity, cross-linked with Genipin
NX 1000	Non- cross-linked chitosan meshes having micro-channels of 1000 µm diameter
NX 500	Non -cross-linked chitosan meshes having micro-channels of 500 µm diameter
NX Random	Non -cross-linked chitosan meshes having a random porosity

their dimensional (3D) cell organization such as cardiac, skeletal, and smooth muscle.[10] For instance, within the heart, cardiomyocytes are organized in interconnected cardiac myofibers that contract synchronously,[11] whereas skeletal muscle is formed by parallel multinucleate myofibers.

All these studies, based on the contact guidance theory,[12] confirm that cells are well equipped to sense some environmental micro- and nano-scale geometric parameters like molecular structure, surface topography, and fiber diameter. Moreover the combination of different factors in the micro-scale environment contribute to the overall control of the new tissue formation.[13-15] For example, surface mechanical properties are of particular relevance for the functionality of contractile cells,[13,14] and this translates into the coupling to a soft or stiff substrate. Many studies have been performed to understand how topographical cues, such as micro-grooves, micropatterns but also micro- and nanofibers, can affect cells behavior for a variety of cell lines and stem cells.[15-20]

The advances in fabrication technology have refined the tools available to create micro- and nano- structured materials and enabled the successful fabrication of a variety of scaffolds that can take advantage of contact guidance in determining the cell fate.

For the fabrication of tissue engineering scaffolds, biodegradable polymers that degrade in tissue over a desired period of time are generally turned to. Biodegradable polymer conduits and tissue engineering scaffolds were produced using extrusion,[21] fiber bonding,[22] salt leaching, freeze drying,[23,24] and laminating.[25,26] However, micro and nano-fabrication of biodegradable polymers with precise control over surface microarchitecture, topography, and size remains an important challenge.[26]

Here we propose an easy method to obtain hierarchical organized CS scaffolds, with highly oriented micro-channels and open micro-pores for tissue engineering applications. These structures have been obtained by a modification of a conventional electrochemical deposition technique where a micro-patterned cathode has been used as positive master. Chitosan membranes prepared with this method have been further cross-linked and characterized in terms of physico-chemical and biological response.

Results

Scaffold morphology

Electrochemical/electrophoretic technique allows the processing of CS and the preparation of cathodic surfaces functionalized with thin films of this biopolymer. All the abbreviations used in the text are resumed in **Table 1**. By fine tuning of process parameters, it is also possible to obtain thick films (up to 2 mm) that can be easily peeled off the cathode metal substrate after freeze drying. With this method, it was possible to obtain CS membranes with two different micro-channels dimensions (1000 and 500 µm in diameter) by using aluminum meshes with a regular lattice of micro-holes, while random porosity (R) films have been deposited on flat aluminum surface. In **Figure 1** the aluminum meshes (A, B) and the morphology of CS films observed by optical microscope (C, D, G) and SEM (E, F, H) are presented. Samples appear homogeneous, with a well-defined morphology. In figure c and d CS samples with micro-channels 1000 and 500 are shown respectively, and, for both, micro-channels are well defined and equally spaced, accurately reproducing the geometry of the aluminum grids used as cathode. Together with the oriented and regularly organized micro-channels (macro-pores) replicating the lattice of substrate patterning (**Fig. 1A and B**), the presence of micro-pores can be also noticed, due to H_2 bubble evolution.[27] In **Figure 1G and H** CS samples deposited on flat surfaces are shown, and as it can be observed, they appear homogeneous, with random porosity created by H_2 bubbles evolution and pores with different dimensions.

For scaffold cross-linking, two different agents have been evaluated: genipin (GEN) and epichlorohydrin (EPI). In **Figure 2**, SEM micrographs of cross-linked specimens are shown: it is possible to notice that the resulting morphology after crosslinking has not been affected. Samples are still homogeneous, with well-defined micro-channels and micro-porosity, no signs of cracks and no changes in micro-channels dimensions being detectable. At optical observation (not shown) Genipin cross-linked scaffolds became blue after cross-linking; it is a typical effect of genipin reaction with amino groups and a qualitatively demonstration of the effectiveness of the cross-linking.[28]

Swelling behavior has been investigated at two different pHs: in PBS at pH 7.4 (mimicking physiological-like conditions) and

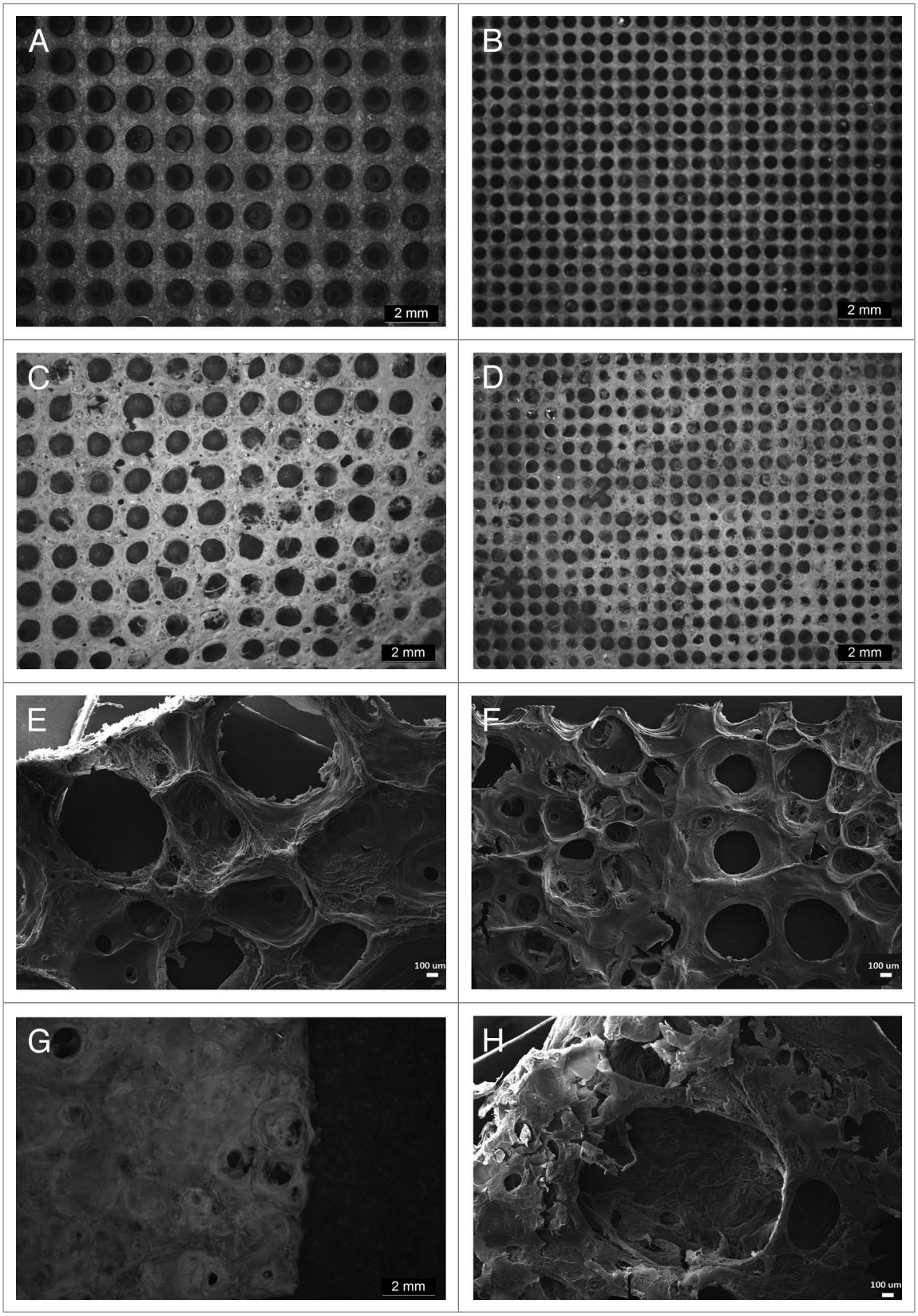

Figure 1. Optical microscope observation of aluminum grids 1000μm microchannels (**A**) and 500μm microchannels; optical and SEM observation of chitosan meshes 1000μm microchannels (**C and E**), 500μm microchannels (**D and F**), random porosity (**G and H**). Scale bar: optical microscope 2 mm, SEM 100 μm.

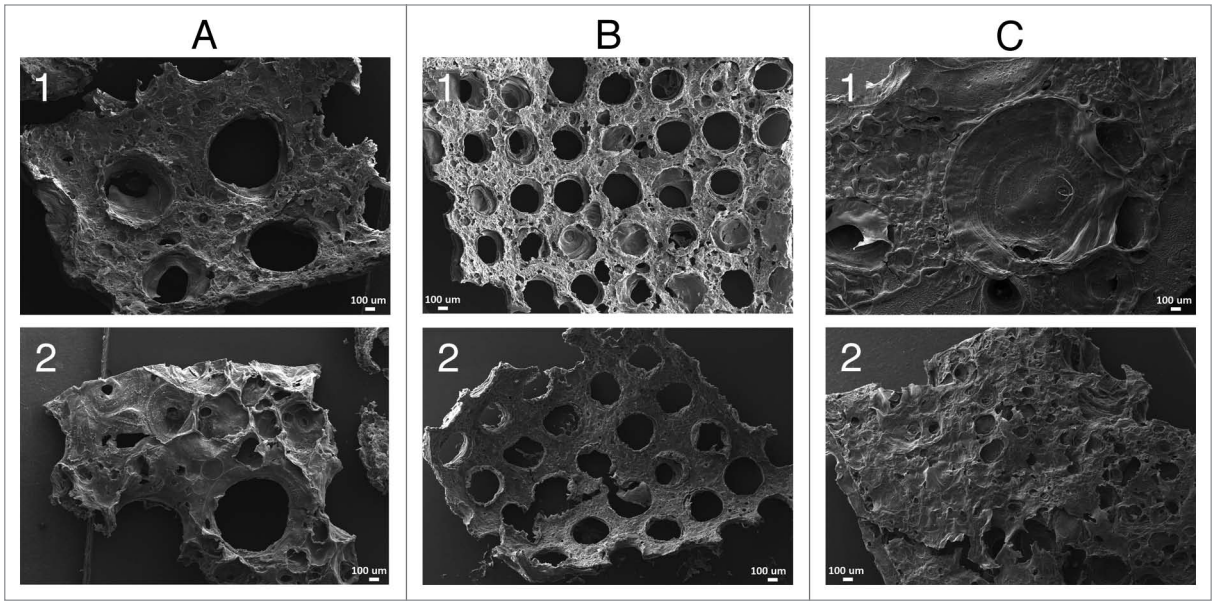

Figure 2. SEM images of Genipin (1) and Epichloroydrin (2) cross-linked meshes with different morphologies 1000μm microchannels (**A**), 500μm microchannels (**B**), random porosity (**C**). Scale bar 100 μm.

in Acetic Acid at pH 5 (mimicking a more aggressive environment such as the oral cavity). **Figure 3** shows water uptake behavior for different scaffold morphologies, cross-liking agent and solution pHs, as fluid absorption rate vs. time. From these plots, it is possible to notice, in each case, a drastic change occurring in the first ten minutes; after this critical period, the absorption reaches a plateau. Non cross-linked (NX) meshes show a higher water uptake for both pHs, while sample morphology did not seem to affect swelling behavior (**Fig. 3A and B**). At pH 7.4 non cross-linked samples swell around 400%, while both EPI samples and GEN samples increase their weight about 300%. This behavior is even more evident at pH 5 (**Fig. 3D**): NX samples swell more than 500% while EPI and GEN samples less than 300%.

Mechanical tests

Mechanical properties have been investigated by tensile tests at a strain rate of 0.2 min^{-1} in wet conditions. Stress, strain at break, and Young modulus are resumed in **Table 2**: results have been analyzed by performing one-way ANOVA and *t* tests (level of confidence $P = 0.05$). 2D geometry seems to have a negligible effect ($P > 0.05$) on non-cross-linked meshes: both elastic moduli and strain at break are comparable. For random specimens, elongation at break is lower and elastic modulus higher for cross-linked specimens vs. NX specimens: however, these differences are negligible ($P > 0.05$). Significant difference ($P < 0.05$) are evidenced only for GEN patterned specimens, in which $\varepsilon_{max}(\%) = (22.4 \pm 5.7)\%$ (GEN500) and $\varepsilon_{max}(\%) = (24.5 \pm 8.2)\%$ (GEN1000) *vs.* $\varepsilon_{max}(\%) = (53.1 \pm 12.5)\%$ (NX500) and $\varepsilon_{max}(\%) = (54.7 \pm 12.6)\%$ (NX1000). Moreover an increase in Elastic Modulus $E = (1.3 \pm 0.3)$ MPa (GEN500) and $E = (1.6 \pm 0.3)$ MPa (GEN1000) vs. $E = (1.12 \pm 0.4)$ MPa (NX500) and $E = (0.8 \pm 0.3)$ MPa (NX1000) was detected. These differences are more pronounced by comparing patterned GEN cross-linked specimens vs. random NX specimens. On the contrary, differences are negligible for EPI crosslinking.

Cytotoxicity

MS1 mouse endothelial cells have been seeded and cultured on samples with both cross-linking agents and all different morphologies, using non-cross- linked samples as control. In **Figure 4** results of MTT cells viability assays at 24h (**Fig. 4A**) and 72h (**Fig. 4B**) after seeding are shown. All materials showed high cell viability with no significant differences for different cross-linking agents. Both classes of cross-linked samples show viability values comparable to non-cross-linked scaffold: 72 h after seeding (**Fig. 4B**) an increase in cells viability has been observed, symptom of a cells proliferation on all samples. MTT results have been confirmed by SEM observations; in **Figure 5**, as an example, cells cultured for 72h on CS scaffolds, with the same morphology, cross-linked with GEN and EPI and NX are shown. Cells are well spread all over the samples and no differences have been noticed imputable to cross-linker agent for all the geometries. To better appreciate cells on the samples a control without cells is shown in **Figure 5D**, showing a very smooth surface compared with samples having cells seeded on.

Discussion

Substrate replica and micro-structuring of scaffolds via electrochemical deposition

Electrochemical and Electrophoretic Depositions (ECD/EPD) are powerful technique to fabricate organic coating. They have been largely investigated in the biomaterials field[29,30] for the deposition of chitosan,[27,31] CaP,[32,33] alginate,[34] Bioglass,[35] different polymer blends, and even hybrid composites.[34-37] Here we decided to further exploit this technique in order to investigate

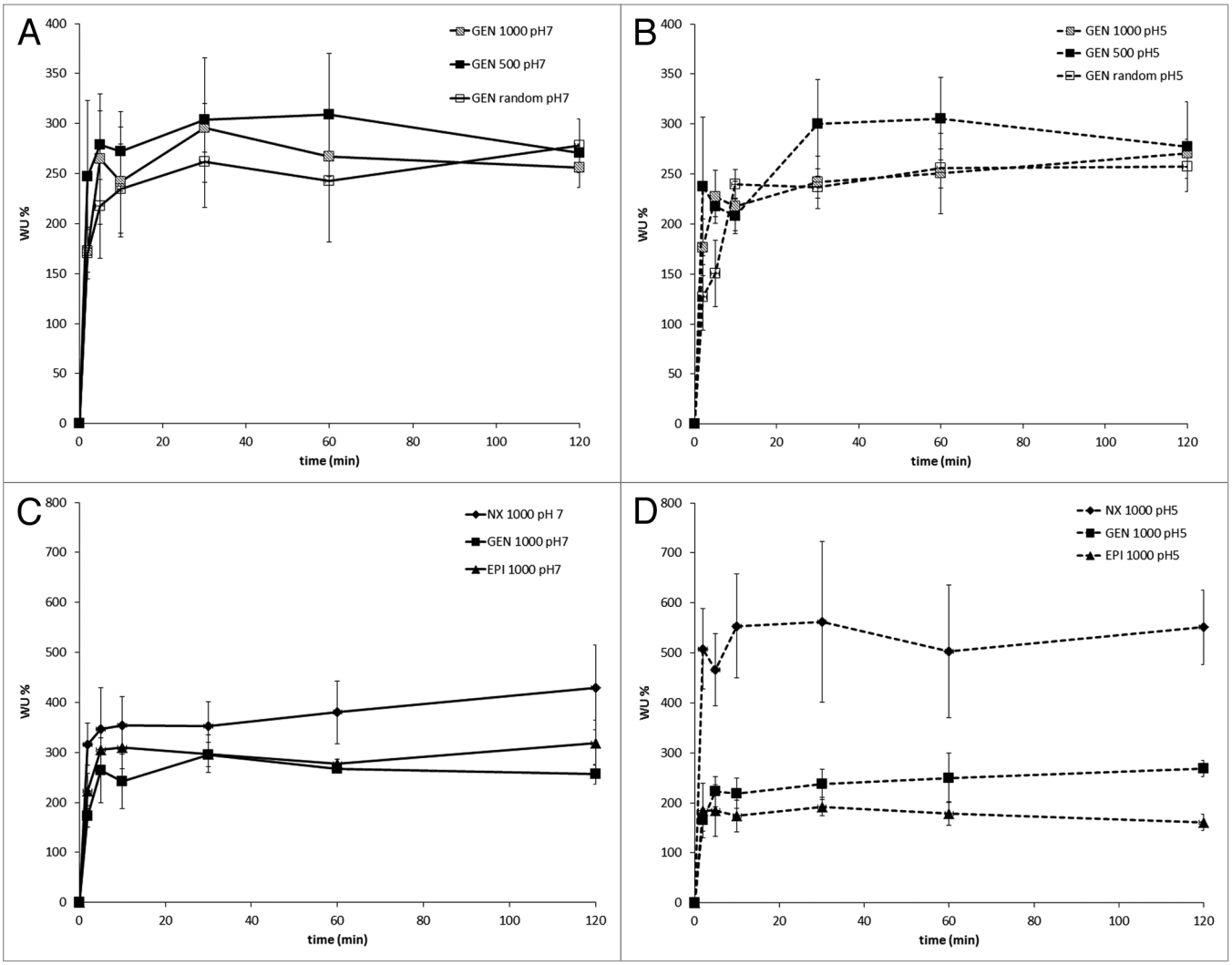

Figure 3. Swelling behavior of CS meshes at pH 7.4 (**A–C**) and at pH 5 (**B–D**), different morphologies (**A–B**), different cross-linker (**C–D**).

the possibility of fabricating porous scaffolds with hierarchical structures characterized by 2D lattice micro-hole patterning and a random micro-porosity. As observed in a previous work, ECD allows the fabrication of chitosan scaffolds with porosity that can be tuned by acting on deposition parameters.[27] Namely, morphological properties of ECD chitosan films can be easily tuned by a suitable selection of anionic species and their concentration, resulting in pore interconnection and dimension in the range of interest for tissue engineering scaffolds. Coupling these results with the use of a patterned cathode, the technique proposed here allows a flexible design and realization of 2D hierarchical structures, and offers the opportunity to realize hierarchical structures using a wide number and types of patterns via conventional micro fabrication technologies of metals. The method here developed can be ascribed to the scaffold fabrication technologies based on substrate replication,[26] the underlying principle being the replication of a micro-fabricated master, that in our case is represented by the cathode, that has a positive pattern to be replicated by the deposition process. The method is quite economic, because the expensive micro-fabrication step is only necessary for the initial fabrication of the master that the electrochemical process allows to replicate several times onto Chitosan. For all the above mentioned reasons, the use of ECD appears as a simple, fast, and effective technique, when compared with other micro-patterning and/or bottom-up technologies, to obtain hierarchical structures. Moreover, the approach here proposed can be easily adopted for all the other materials that have been processed via ECD/EPD,[27,29,30,33,34,38,39] Chitosan having being selected for this work as a model polymer.

Modulation of chemico-physical properties via chemical crosslinking

Robust Chitosan hydrogel can be produced via chemical covalent crosslinking, either by using small cross-linker molecules, secondary polymerization, or irradiation chemistry.[40] Irreversible polymer networks can be realized hence by bond small molecules to $-NH_2$ or $-OH$ groups in the chitosan backbone: according to one of these strategies and given a certain degree of deacetylation of the Chitosan, different level of free amino-groups will result. In order to modulate the free amino-groups, here we used two different cross-linker agents, namely genipin and epichlorohydrin.

Table 2. Mechanical properties: elongation at break (ε [%]); Young modulus E (MPa). Statistical analysis show significant differences ($P < 0.05$ at t test) for: Young Modulus GEN1000 vs NX1000 and GEN500 vs NX500; ε at break GEN1000 vs NX1000 and GEN500 vs NX500

Sample type	ε (%)	E (MPa)
EPI 1000	41.4 ± 7.2	1.1 ± 0.3
EPI 500	33.6 ± 12.3	0.7 ± 0.2
EPI Random	56.4 ± 14.0	1.0 ± 0.5
GEN 1000	24.5 ± 8.2	1.6 ± 0.3
GEN 500	22.4 ± 5.7	1.33 ± 0.3
GEN Random	43.3 ± 13.6	1.1 ± 0.6
NX 1000	54.7 ± 12.5	0.8 ± 0.2
NX 500	53.1 ± 12.5	1.1 ± 0.4
NX Random	60.2 ± 13.9	0.7 ± 0.1

Genipin has been widely used in biomedical field due to its low cytotoxicity compared with other cross-linking agents, such as glutaraldehyde,[28,41-43] while Epichlorohydrin has been used due to the ability of bond –OH groups that results in free amino group.[44,45] The cross-linking mechanisms of the two selected molecules are indeed different: genipin carboxymethyl groups first react with amino groups of Chitosan to form secondary amide, then nucleophilic attack by amino groups of Chitosan on the olefinic carbon atom at C-3 of deoxyloganin aglycone followed by the opening of the dihydropyran ring to form heterocyclic amine.[28,46] Epichlorohydrin reacts with Chitosan hydroxyl group under alkaline condition, resulting in free cationic amine functions of Chitosan: the resulting material shows excellent adsorption properties of anionic dyes strongly attracted by electrostatic forces in the acidic media.[44,45,47]

The chemical crosslinking of Chitosan films strongly depends on both the used chemical reagents and the crosslinking conditions. Here the obtained 3D membranes were removed from the deposition cathode masks and then immersed in a crosslinking bath. According to the definition of Cao et al., this crosslinking procedure is a surface cross-linking approach (or heterogeneous crosslinking)[48]: heterogeneous approach, when compared with homogeneous one, allows to obtain structures with lower amount of unreacted cross-linking agents left in the polymer and to maintain the desired shape.

By combining a suitable selection of chemical cross-linkers and the processing procedure, we were able to maintain the obtained 3D shape and to modulate the swelling behavior. In facts, even if no difference has been noticed between the two cross-linking agents in terms of the swelling behavior, when compared with non-cross-linked specimens, both GEN and EPI resulted in a lower water uptake.[24,42,49]

The comparison of the obtained results with published data appears however difficult, probably due to the particular morphology of our samples, having a random and an oriented porosity that should affect the swelling behavior. Reported swelling ratio data are both higher[24,49] and lower[42,43]when compared with here reported data. Jin et al.[42] performed a detailed study on differences in swelling ratio depending on the pH and the genipin concentrations, by showing a great variability in swelling ratio. The particular morphology and the lower percentage of genipin probably allow for a higher swelling ratio in our sample compared with other studies.[41,43]

Cao et al.[48] cross-linked chitosan films with hexamethylene diisocyanate (HDI), epichlorohydrin (ECH) and glutaraldehyde (GA); in this case, they used smooth films, so probably the different swelling behavior of our scaffold can be again ascribed to the porosity. Garnica-Palafox et al.[50] studied a hybrid hydrogel based on chitosan and poly(vinyl alcohol), chemically cross-linked with epichlorohydrin, in this case the higher swelling ratio we found should depend both on the presence of PVA but also on the cross-linking performed in bulk conditions.

These differences in absolute values in water uptake can be correlated with the crystallinity degree, crosslinking degree, and 3D morphology of the Chitosan cellular solids. For chitosan membranes, the swelling properties are simultaneously controlled by both the crystallinity and crosslinking. Moreover, the crystalline structure can be influenced by the crosslinking, resulting in a complex and difficult to predict behavior.[48,51] Finally, the morphology of our samples, having a random or an oriented porosity, should dramatically affect the swelling behavior.

Mechanical properties

For non-patterned non-cross-linked Chitosan films, data obtained in this work result lower in terms of E modulus and higher in terms of elongation at break (**Table 2**). These results can be correlated with the lower density of our samples[27] compared with the values commonly found in literature. In refs. 41, 48, and 50 higher values of mechanical properties have been found, probably due to the non-porous structure of the samples. The elongation at break, on the contrary, is higher for our samples; this behavior could be ascribed to the morphology: in fact the presence of a porous structure allows higher deformations. This trend (increase in strain at break and decrease of E modulus) is also reported for chitosan foams obtained with different techniques: Madihally and Matthew[23] report, for instance, that while non-porous chitosan membranes exhibit a maximum strain of 30–40%, porous scaffolds are more extensible, with maximum strain ranging from 30% to 100% as a function of pore orientation and pore diameters. Moreover, Kjm et al.[52] reported tensile strength values higher than here reported: however this result should be ascribed to the porosity of our samples, but also to de different test condition (wet vs. dry) that are unspecified in the cited paper.

Micropatterning for non-cross-linked specimens do not seem to affect ($P > 0.05$) the resulting mechanical properties, both in terms of elastic moduli and maximum strains. The effects of mechanical properties of 2D solids can be found in different previous published works, and in a complete and comprehensive way in L. Gibson book.[53] However, the behavior of such structures is strongly affected, from a mechanical point of view, by the presence of defects. Even if our procedure has been optimized, cracks, notches and holes (due also to the electrochemical deposition process) are evident. As shown by Andrews and Gibson,[54] the overall system response is complex, in some cases resulting in strengthening effects of defects: in order to understand the effects

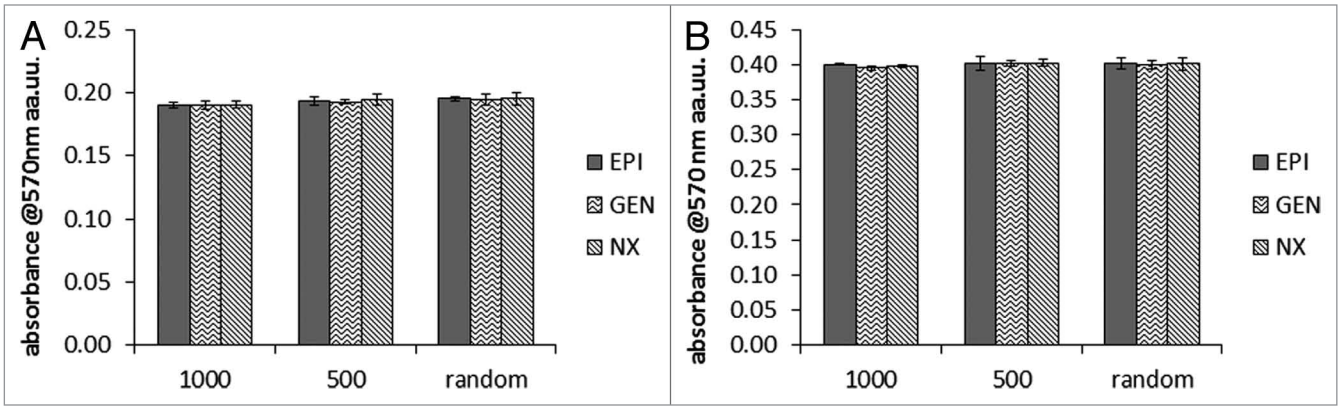

Figure 4. MTT assay of MS1 cells on the different substrata 24h (**A**) and 72h (**B**) after seeding.

of micro-patterning on mechanical properties will be hence necessary to evaluate them by mechanics of solids tools taking into account the effects of the presence of defects. Moreover, as previously pointed out, Chitosan mechanical properties strongly depends on the degree of crystallinity: the electrochemical process and the cathode patterning should affect the mechanisms of coagulation and hence final crystallinity of the structure.

Crosslinking of chitosan plays a pivotal role also in modulation of mechanical properties[28,48,51,52] and it has been used in order to make the material suitable for the desired application. Even if mechanical strength of a hydrogel is often derived almost entirely from the cross-links in the system,[55] the effects of chemical crosslinkers on the resulting mechanical properties in Chitosan are complex, depending also on the process conditions. For instance, the crystallinity degree is affected by a homogeneous crosslinking procedure, which results in its significant decrease when compared with heterogeneous approach.[51]

From a statistical point of view, significant differences have been found ($P < 0.05$) in micro-patterned genipin cross-linked specimens, when compared with non-cross-linked and random specimens, both in terms of Elastic moduli and strain at break: behavior is coherent with expected trends, i.e., increase in E and decrease in maximum strain. The more pronounced effects on micro-patterned structures could be ascribed to the selected heterogeneous crosslinking approach: the overall surface/volume ratios result higher for micro-patterned specimens, probably allowing a higher degree of cross-linking.

The negligible effects from a mechanical point of view, both in elongation at break and elastic modulus for EPI cross-linked specimens is in accordance with previously published data.[51] Wan et al. report that in heterogeneous crosslinking, mechanical properties are almost unchanged (in the experimental error of the measurement) when the concentration of crosslinking agent is low. Value of concentration of crosslinking becomes significant, in order to affect the mechanical properties, above 0.02 mol for EPI, that is higher than the value here used.

Cytotoxicity tests

Both cross-linked meshes resulted not cytotoxic. Genipin has been largely used due to the low cytotoxicity compared, for example, to glutaraldehyde,[49,56] these results being confirmed by our study.

Reported data on cytotoxicity on epichlorohydrin is poor and controversial.[48,50,57] Nevertheless, we decided to investigate the use of epichlorohydrin in order to obtain chitosan networks with free amino-groups. A heterogeneous cross-linking procedure, and a careful washing, have been used in order to minimize the unreacted traces of chemical reagent. Both the surface cross-linking and the washing procedure assured us a good cytocompatibility of our meshes; in heterogeneous approach chitosan is cross-linked as swollen solid, molecules hardly diffuse through the membrane[51] and the unreacted species are probably easily removed from a suitable washing procedure. According to Garnica-Palafox et al.,[50] washing procedure is a critical step in epichlorohydrin removal.

Conclusions

In this work, we showed a simple and effective method based on electrochemical deposition of Chitosan onto patterned cathodes used as positive replica substrates to obtain 2D scaffolds with oriented and highly ordered micro-channels. Chitosan structures are easily peeled off from the cathode and could be used as self-standing structures or to fabricate 3D scaffolds with oriented porosities. We further cross-linked obtained meshes by using genipin and epichlorohydrin with a heterogeneous approach that resulted in negligible morphological effects. According to the crosslinking mechanisms, either cross-linking agent could be selected depending on the envisaged applications: epichlorohydrin in applications in which free amino-groups requested, genipin for free hydroxyl group. These new 2D scaffolds can be easily cross-linked, and this process affected only slightly the mechanical properties, without compromising the cytocompatibility.

Thanks to the possibility of controlling the porosity and the micro-channel orientation, these structures are extremely promising for different tissue engineering applications especially in

regeneration of tissues that requires a preferential cells orientation, such as cardiac patches or ligament regeneration.

Materials and Methods

Chitosan (CS) 2D scaffolds with oriented porosity have been fabricated by cathodic polarization on aluminum grids (2 × 2 cm^2) used as cathode. Two different laser cut aluminum grids have been used: one with circular pores of diameter equal to 500 μm and wheelbase of 700 μm and the other with pores of a diameter of 1000 μm and wheelbase of 1500 μm. A flat aluminum foil was also used as control to fabricate 2D scaffolds with random porosity. Cathodic deposition was performed in galvanostatic condition at 6.75 mA cm^{-2} in an electrolytic bath of Chitosan from shrimp shell (Sigma-Aldrich 417963, lot MKBC3804, 75–85% deacetylated) 0.1% (w/v) in acetic acid (ACS reagent, ≥99.7%, Sigma-Aldrich 320099) at pH 3.5. After deposition, samples have been washed three times in deionized water and freeze-dried to easily peel off the Chitosan meshes from the grid. No weight variations have been observed indicating the presence of acetic acid entrapped in the samples.

Sample preparation

Cross linking

Two different cross-linking agents have been used: Genipin (Sigma-Aldrich G4796) and Epichlorohydrin (Sigma-Aldrich 45340). Meshes with oriented and random pores (1 × 1cm^2) have been immersed in a genipin solution (1% $w_{genepin}/w_{chitosan}$ 0.85 ml cm^{-2}) at 37 °C for 24h. Meshes with oriented and random pores (1 × 1 cm^2) have been immersed in an epichlorohydrin solution (2 cm^2 ml^{-1}) 0.01M in NaOH (Sigma-Aldrich 71690) at pH 10 up to 72h at room temperature. Samples were washed five times in distilled water to remove any residual genipin or epichlorohydrin and then dried at 37 °C overnight, weighted and stored in dry condition at room temperature until further testing.

Morphological characterization

Optic microscopy (LEICA DM LM) and Scanning Electron Microscope (Cambridge Instrument Stereoscan 360) have been used to evaluate the morphology of meshes with oriented and random porosity. Before SEM observation samples were dehydrated by different ethanol concentrations from 25 to 100% v/v and gold sputtered.

Mechanical properties

The dried specimens (five for each type) were cut into rectangular shapes (5 × 15mm^2) and left to swell for 24h in PBS (Sigma-Aldrich D8537) at 37 °C. Tensile tests have been performed on swollen samples at room temperature by applying a strain rate of 0.2 min^{-1} by using a Dynamic Mechanical Analyzer (DMA Q800 TA Instrument). Statistical analysis have been performed by one-way ANOVA and *t* test (level of confidence P = 0.05).

Swelling

The swelling properties of CS-meshes were studied by immersing the samples in Phosphate Buffer Solution (PBS) (pH 7.4) at 37 °C, and in Acetic Acid at pH 5 at room temperature. The dried meshes (four for each type) were cut into small squares

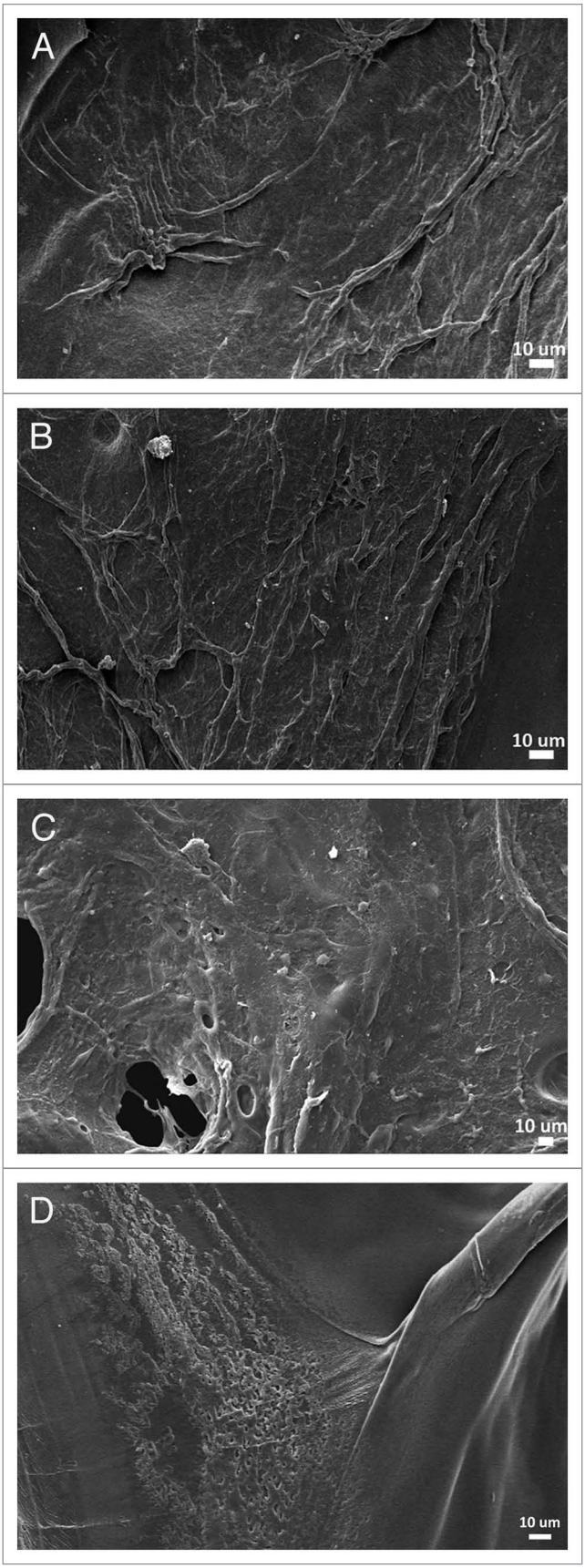

Figure 5. SEM images of MS1 cells cultured for 72h on different chitosan scaffolds: GEN1000 (**A**); EPI1000 (**B**); NX1000 (**C**); scaffolds without cells (**D**).

with 10 mm by side. At predetermined intervals of time (2, 5, 10, 30, 60, 120 min), the specimens were removed from the solutions and carefully dried using filter paper. The free water was removed so that the interstitial water was trapped only in the polymer network. Subsequently, the samples were weighted and then returned to the same container until the equilibrium was reached. The percentage of water uptake (WU) was calculated using the following equation

$$WU = 100 * \frac{ws - wd}{wd} \quad (1)$$

where w_s is the weight of swollen hydrogel at different swelling time and w_d corresponds to the weight before hydration.

Cytotoxicity test

MS1 mouse endothelial cells (ATCC CRL-2279) were cultivated in Dulbecco's Modified Eagle Medium (DMEM, Sigma-Aldrich D5671) supplemented with 10% fetal bovine serum (FBS, Sigma-Aldrich F4165) and antibiotics (1% penicillin/streptomycin, Sigma-Aldrich P4333). At about 80% confluence, cells were detached by trypsin/EDTA solution and used for experiments.

For the direct contact assay, samples were immersed in ethanol solution (70% v/v) for 30 min and then washed three times in sterile PBS. Cells were seeded in a defined number (3×10^4 / sample) directly onto the surfaces of each samples and cultivated in DMEM + 10% FBS at 37 °C, 5% CO_2. Cells viability was evaluated after 24 and 72 h with the 3-(4,5-dimethylthiazol-2-yl)-2,5-diphenyltetrazolium bromide colorimetric assay (MTT, Sigma-Aldrich M5655). Briefly, 100 μl of MTT solution (3 mg/ml in phosphate buffered saline (PBS, pH 7.4) were added to each sample and incubated 4 h in the dark; afterwards, formazan crystals were solved with 100 μl of dimethyl sulphoxyde (DMSO, Sigma-Aldrich 154938) and 50 μl were collected and centrifuged to remove eventually debris. Surnatant optical density (o.d.) was evaluated at 570 nm with a spectrophotometer (Spectra Count, Packard Bell). Not cross-linked samples o.d. was used as control and considered as 100% cells viability, while cross-linked samples viability was calculated as follow:

$$100 * \frac{sample\ o.d.}{control\ o.d.} \quad (2)$$

Experiments were performed in triplicate.

For the indirect test, the tested material (controls or cross-linked samples, circular shape, 5 mm diameter) were incubated in direct contact with 1 ml of serum-free DMEM without cells for 1 wk at 37 °C, 5% CO_2. Afterwards, eluates were collected, supplemented with 10% FBS and used to cultivate mouse endothelial cells. Cells were seeded in a defined number (3×10^4 / well) into 24 wells plates (Cell Star, PBI International) and cultivated for 24 and 72 h at 37 °C, 5% CO_2. Afterwards, cells viability was evaluated by the MTT test as described in the direct contact test. Experiments were performed in triplicate.

Direct contact cytocompatibility was also visually investigated by morphological observation of cells cultivated directly onto samples surfaces with SEM. Samples after 24 and 72 h of culture were washed gently with PBS and fixed with a solution of 4% formaldehyde and 3% sucrose in PBS. Afterwards samples were washed in Sodium Cacodylate solution at pH 7.4 (Sodium Cacodylate Trihydrate, Fluka 20840) and a standard dehydration procedure based on different ethanol concentrations (from 25 to 100% v/v) was made before SEM observations.

Disclosure of Potential Conflicts of Interest

No potential conflicts of interest were disclosed.

Acknowledgments

L.A. and L.D. thank: MIUR-FIRB Futuro in ricerca (Surface-associated selective transfection - SAST, RBFR08XH0H) for the economic support; Dr M. Moscatelli for help in statistical analysis and Dr L. Draghi for English revision.

References

1. Bouten CV, Dankers PY, Driessen-Mol A, Pedron S, Brizard AM, Baaijens FP. Substrates for cardiovascular tissue engineering. Adv Drug Deliv Rev 2011; 63:221-41; PMID:21277921; http://dx.doi.org/10.1016/j.addr.2011.01.007
2. Yi BA, Wernet O, Chien KR. Pregenerative medicine: developmental paradigms in the biology of cardiovascular regeneration. J Clin Invest 2010; 120:20-8; PMID:20051633; http://dx.doi.org/10.1172/JCI40820
3. Zimmermann WH, Melnychenko I, Wasmeier G, Didié M, Naito H, Nixdorff U, Hess A, Budinsky L, Brune K, Michaelis B, et al. Engineered heart tissue grafts improve systolic and diastolic function in infarcted rat hearts. Nat Med 2006; 12:452-8; PMID:16582915; http://dx.doi.org/10.1038/nm1394
4. Alcon A, Cagavi Bozkulak E, Qyang Y. Regenerating functional heart tissue for myocardial repair. Cell Mol Life Sci 2012; 69:2635-56; PMID:22388688; http://dx.doi.org/10.1007/s00018-012-0942-4
5. Slaughter BV, Khurshid SS, Fisher OZ, Khademhosseini A, Peppas NA. Hydrogels in regenerative medicine. Adv Mater 2009; 21:3307-29; PMID:20882499; http://dx.doi.org/10.1002/adma.200802106
6. Mano JF, Silva GA, Azevedo HS, Malafaya PB, Sousa RA, Silva SS, Boesel LF, Oliveira JM, Santos TC, Marques AP, et al. Natural origin biodegradable systems in tissue engineering and regenerative medicine: present status and some moving trends. J R Soc Interface 2007; 4:999-1030; PMID:17412675; http://dx.doi.org/10.1098/rsif.2007.0220
7. Kim IY, Seo SJ, Moon HS, Yoo MK, Park IY, Kim BC, Cho CS. Chitosan and its derivatives for tissue engineering applications. Biotechnol Adv 2008; 26:1-21; PMID:17884325; http://dx.doi.org/10.1016/j.biotechadv.2007.07.009
8. Lü S, Wang H, Lu W, Liu S, Lin Q, Li D, Duan C, Hao T, Zhou J, Wang Y, et al. Both the transplantation of somatic cell nuclear transfer- and fertilization-derived mouse embryonic stem cells with temperature-responsive chitosan hydrogel improve myocardial performance in infarcted rat hearts. Tissue Eng Part A 2010; 16:1303-15; PMID:19905874; http://dx.doi.org/10.1089/ten.tea.2009.0434
9. Lu WN, Lü SH, Wang HB, Li DX, Duan CM, Liu ZQ, Hao T, He WJ, Xu B, Fu Q, et al. Functional improvement of infarcted heart by co-injection of embryonic stem cells with temperature-responsive chitosan hydrogel. Tissue Eng Part A 2009; 15:1437-47; PMID:19061432; http://dx.doi.org/10.1089/ten.tea.2008.0143
10. Motlagh D, Senyo SE, Desai TA, Russell B. Microtextured substrata alter gene expression, protein localization and the shape of cardiac myocytes. Biomaterials 2003; 24:2463-76; PMID:12695073; http://dx.doi.org/10.1016/S0142-9612(02)00644-0
11. Deutsch J, Motlagh D, Russell B, Desai TA. Fabrication of microtextured membranes for cardiac myocyte attachment and orientation. J Biomed Mater Res 2000; 53:267-75; PMID:10813767; http://dx.doi.org/10.1002/(SICI)1097-4636(2000)53:3<267::AID-JBM12>3.0.CO;2-J
12. Curtis A, Wilkinson C. Topographical control of cells. Biomaterials 1997; 18:1573-83; PMID:9613804; http://dx.doi.org/10.1016/S0142-9612(97)00144-0
13. Engler AJ, Griffin MA, Sen S, Bönnemann CG, Sweeney HL, Discher DE. Myotubes differentiate optimally on substrates with tissue-like stiffness: pathological implications for soft or stiff microenvironments. J Cell Biol 2004; 166:877-87; PMID:15364962; http://dx.doi.org/10.1083/jcb.200405004
14. Ingber DE. Mechanical control of tissue growth: function follows form. Proc Natl Acad Sci U S A 2005; 102:11571-2; PMID:16091458; http://dx.doi.org/10.1073/pnas.0505939102

15. Choi YS, Vincent LG, Lee AR, Kretchmer KC, Chirasatitsin S, Dobke MK, Engler AJ. The alignment and fusion assembly of adipose-derived stem cells on mechanically patterned matrices. Biomaterials 2012; 33:6943-51; PMID:22800539; http://dx.doi.org/10.1016/j.biomaterials.2012.06.057
16. Bayati V, Altomare L, Tanzi MC, Farè S. Adipose-derived stem cells could sense the nano-scale cues as myogenic-differentiating factors. J Mater Sci Mater Med 2013; 24:2439-47; PMID:23793565; http://dx.doi.org/10.1007/s10856-013-4983-5
17. Altomare L, Gadegaard N, Visai L, Tanzi MC, Farè S. Biodegradable microgrooved polymeric surfaces obtained by photolithography for skeletal muscle cell orientation and myotube development. Acta Biomater 2010; 6:1948-57; PMID:20040385; http://dx.doi.org/10.1016/j.actbio.2009.12.040
18. Altomare L, Riehle M, Gadegaard N, Tanzi MC, Farè S. Microcontact printing of fibronectin on a biodegradable polymeric surface for skeletal muscle cell orientation. Int J Artif Organs 2010; 33:535-43; PMID:20872348
19. Beier JP, Klumpp D, Rudisile M, Dersch R, Wendorff JH, Bleiziffer O, Arkudas A, Polykandriotis E, Horch RE, Kneser U. Collagen matrices from sponge to nano: new perspectives for tissue engineering of skeletal muscle. BMC Biotechnol 2009; 9:34; PMID:19368709; http://dx.doi.org/10.1186/1472-6750-9-34
20. Huang NF, Patel S, Thakar RG, Wu J, Hsiao BS, Chu B, Lee RJ, Li S. Myotube assembly on nanofibrous and micropatterned polymers. Nano Lett 2006; 6:537-42; PMID:16522058; http://dx.doi.org/10.1021/nl060060o
21. Widmer MS, Gupta PK, Lu L, Meszlenyi RK, Evans GRD, Brandt K, Savel T, Gurlek A, Patrick CW Jr., Mikos AG. Manufacture of porous biodegradable polymer conduits by an extrusion process for guided tissue regeneration. Biomaterials 1998; 19:1945-55; PMID:9863528; http://dx.doi.org/10.1016/S0142-9612(98)00099-4
22. Mikos AG, Bao Y, Cima LG, Ingber DE, Vacanti JP, Langer R. Preparation of poly(glycolic acid) bonded fiber structures for cell attachment and transplantation. J Biomed Mater Res 1993; 27:183-9; PMID:8382203; http://dx.doi.org/10.1002/jbm.820270207
23. Madihally SV, Matthew HWT. Porous chitosan scaffolds for tissue engineering. Biomaterials 1999; 20:1133-42; PMID:10382829; http://dx.doi.org/10.1016/S0142-9612(99)00011-3
24. Bi L, Cao Z, Hu Y, Song Y, Yu L, Yang B, Mu J, Huang Z, Han Y. Effects of different cross-linking conditions on the properties of genipin-cross-linked chitosan/collagen scaffolds for cartilage tissue engineering. J Mater Sci Mater Med 2011; 22:51-62; PMID:21052794; http://dx.doi.org/10.1007/s10856-010-4177-3
25. Mikos AG, Sarakinos G, Leite SM, Vacanti JP, Langer R. Laminated three-dimensional biodegradable foams for use in tissue engineering. Biomaterials 1993; 14:323-30; PMID:8507774; http://dx.doi.org/10.1016/0142-9612(93)90049-8
26. Lu Y, Chen SC. Micro and nano-fabrication of biodegradable polymers for drug delivery. Adv Drug Deliv Rev 2004; 56:1621-33; PMID:15350292; http://dx.doi.org/10.1016/j.addr.2004.05.002
27. Altomare L, Draghi L, Chiesa R, De Nardo L. Morphology tuning of chitosan films via electrochemical deposition. Mater Lett 2012; 78:18-21; http://dx.doi.org/10.1016/j.matlet.2012.03.035
28. Muzzarelli RAA. Genipin-crosslinked chitosan hydrogels as biomedical and pharmaceutical aids. Carbohydr Polym 2009; 77:1-9; http://dx.doi.org/10.1016/j.carbpol.2009.01.016
29. Boccaccini AR, Keim S, Ma R, Li Y, Zhitomirsky I. Electrophoretic deposition of biomaterials. J R Soc Interface 2010; 7(Suppl 5):S581-613; PMID:20504802; http://dx.doi.org/10.1098/rsif.2010.0156.focus
30. Besra L, Liu M. A review on fundamentals and applications of electrophoretic deposition (EPD). Prog Mater Sci 2007; 52:1-61; http://dx.doi.org/10.1016/j.pmatsci.2006.07.001
31. Simchi A, Pishbin F, Boccaccini AR. Electrophoretic deposition of chitosan. Mater Lett 2009; 63:2253-6; http://dx.doi.org/10.1016/j.matlet.2009.07.046
32. Redepenning J, Venkataraman G, Chen J, Stafford N. Electrochemical preparation of chitosan/hydroxyapatite composite coatings on titanium substrates. J Biomed Mater Res A 2003; 66:411-6; PMID:12889012; http://dx.doi.org/10.1002/jbm.a.10571
33. Altomare L, Visai L, Bloise N, Arciola CR, Ulivi L, Candiani G, Cigada A, Chiesa R, De Nardo L. Electrochemically deposited gentamicin-loaded calcium phosphate coatings for bone tissue integration. Int J Artif Organs 2012; 35:876-83; PMID:23138703
34. Chen Q, Cordero-Arias L, Roether JA, Cabanas-Polo S, Virtanen S, Boccaccini AR. Alginate/Bioglass® composite coatings on stainless steel deposited by direct current and alternating current electrophoretic deposition. Surf Coat Tech 2013; 233:49-56; http://dx.doi.org/10.1016/j.surfcoat.2013.01.042
35. Pishbin F, Simchi A, Ryan MP, Boccaccini AR. Electrophoretic deposition of chitosan/45S5 Bioglass (R) composite coatings for orthopaedic applications. Surf Coat Tech 2011; 205:5260-8; http://dx.doi.org/10.1016/j.surfcoat.2011.05.026
36. Pishbin F, Simchi A, Ryan MP, Boccaccini AR. A study of the electrophoretic deposition of Bioglass (R) suspensions using the Taguchi experimental design approach. J Eur Ceram Soc 2010; 30:2963-70; http://dx.doi.org/10.1016/j.jeurceramsoc.2010.03.004
37. Li Y, Pang X, Epand RF, Zhitomirsky I. Electrodeposition of chitosan-hemoglobin films. Mater Lett 2011; 65:1463-5; http://dx.doi.org/10.1016/j.matlet.2011.02.038
38. Seuss S, Boccaccini AR. Electrophoretic deposition of biological macromolecules, drugs, and cells. Biomacromolecules 2013; 14:3355-69; PMID:24001091; http://dx.doi.org/10.1021/bm401021b
39. De Nardo L, Altomare L, Del Curto B, Cigada A, Draghi L. Electrochemical surface modifications of titanium and titanium alloys for biomedical applications. In: Driver M, ed. Coatings for Biomedical Applications: Woodhead Publishing, 2012:106-42.
40. Bhattarai N, Gunn J, Zhang M. Chitosan-based hydrogels for controlled, localized drug delivery. Adv Drug Deliv Rev 2010; 62:83-99; PMID:19799949; http://dx.doi.org/10.1016/j.addr.2009.07.019
41. Mi FL, Tan YC, Liang HC, Huang RN, Sung HW. In vitro evaluation of a chitosan membrane cross-linked with genipin. J Biomater Sci Polym Ed 2001; 12:835-50; PMID:11718480; http://dx.doi.org/10.1163/156856201753113051
42. Jin J, Song M, Hourston DJ. Novel chitosan-based films cross-linked by genipin with improved physical properties. Biomacromolecules 2004; 5:162-8; PMID:14715022; http://dx.doi.org/10.1021/bm034286m
43. Mi FL, Sung HW, Shyu SS. Synthesis and characterization of a novel chitosan-based network prepared using naturally occurring crosslinker. J Polym Sci 2000; 38:2804-14; http://dx.doi.org/10.1002/1099-0518(20000801)38:15<2804::AID-POLA210>3.0.CO;2-Y
44. Vieira RS, Beppu MM. Interaction of natural and crosslinked chitosan membranes with Hg(II) ions. Colloids Surf A Physicochem Eng Asp 2006; 279:196-207; http://dx.doi.org/10.1016/j.colsurfa.2006.01.026
45. Wang G, Liu J, Wang X, Xie Z, Deng N. Adsorption of uranium (VI) from aqueous solution onto cross-linked chitosan. J Hazard Mater 2009; 168:1053-8; PMID:19342166; http://dx.doi.org/10.1016/j.jhazmat.2009.02.157
46. Mi FL, Shyu SS, Peng CK. Characterization of ring-opening polymerization of genipin and pH-dependent cross-linking reactions between chitosan and genipin. Journal of Polymer Science 2005; 43:1985-2000
47. Liu YH, Cao XH, Hua R, Wang YQ, Liu YT, Pang C, Wang Y. Selective adsorption of uranyl ion on ion-imprinted chitosan/PVA cross-linked hydrogel. Hydrometallurgy 2010; 104:150-5; http://dx.doi.org/10.1016/j.hydromet.2010.05.009
48. Cao W, Cheng M, Ao Q, Gong Y, Zhao N, Zhang X. Physical, mechanical and degradation properties, and schwann cell affinity of cross-linked chitosan films. J Biomater Sci Polym Ed 2005; 16:791-807; PMID:16028597; http://dx.doi.org/10.1163/1568562053992496
49. Tian JS, Cui YL, Yao KD. Ieee. A study on the fabrication of porous scaffold cross-linked with genipin. 2009 3rd International Conference on Bioinformatics and Biomedical Engineering, Vols 1-11 2009:967-70.
50. Garnica-Palafox IM, Sánchez-Arévalo FM, Velasquillo C, García-Carvajal ZY, García-López J, Ortega-Sánchez C, Ibarra C, Luna-Bárcenas G, Solís-Arrieta L. Mechanical and structural response of a hybrid hydrogel based on chitosan and poly(vinyl alcohol) cross-linked with epichlorohydrin for potential use in tissue engineering. J Biomater Sci Polym Ed 2014; 25:32-50; PMID:24007370; http://dx.doi.org/10.1080/09205063.2013.833441
51. Wan Y, Creber KAM, Peppley B, Bui VT. Ionic conductivity and related properties of crosslinked chitosan membranes. J Appl Polym Sci 2003; 89:306-17; http://dx.doi.org/10.1002/app.12090
52. Kjm KM, Son JH, Kim SK, Weller CL, Hanna MA. Properties of chitosan films as a function of pH and solvent type. J Food Sci 2006; 71:E119-24; http://dx.doi.org/10.1111/j.1365-2621.2006.tb15624.x
53. Gibson LJ, Ashby MF. Cellular Solids Structure and Properties. Cambridge Solid State Science Series, 1999.
54. Andrews EW, Gibson LJ. The influence of cracks, notches and holes on the tensile strength of cellular solids. Acta Mater 2001; 49:2975-9; http://dx.doi.org/10.1016/S1359-6454(01)00203-8
55. Anseth KS, Bowman CN, Brannon-Peppas L. Mechanical properties of hydrogels and their experimental determination. Biomaterials 1996; 17:1647-57; PMID:8866026; http://dx.doi.org/10.1016/0142-9612(96)87644-7
56. Pauliukaite R, Ghica ME, Fatibello-Filho O, Brett CMA. Comparative study of different cross-linking agents for the immobilization of functionalized carbon nanotubes within a chitosan film supported on a graphite-epoxy composite electrode. Anal Chem 2009; 81:5364-72; PMID:19473012; http://dx.doi.org/10.1021/ac900464z
57. Chang CY, Chen S, Zhang LN. Novel hydrogels prepared via direct dissolution of chitin at low temperature: structure and biocompatibility. J Mater Chem 2011; 21:3865-71; http://dx.doi.org/10.1039/c0jm03075a